

Diruthenium Phenylacetylide Complexes Bearing *para*-/*meta*-Amino Phenyl Substituents

Steven P. Cummings, Zhi Cao, Carl W. Liskey, Alex R. Geanes, Phillip E. Fanwick, Kerry M. Hassell, and Tong Ren*

Department of Chemistry, Purdue University, 560 Oval Drive, West Lafayette, Indiana 47907

Received April 3, 2010

Presented herein is the synthesis and characterization of four diruthenium(II,III) compounds of formulas $\text{Ru}_2(\text{Xap})_4(\text{C}\equiv\text{C}-\text{C}_6\text{H}_4-4-\text{NH}_2)$ (Xap is 2-anilinopyridinate, **1a**; and 2-(3,5-dimethoxy)-anilinopyridinate, **1b**) and $\text{Ru}_2(\text{Xap})_4(\text{C}\equiv\text{C}-\text{C}_6\text{H}_4-3-\text{NH}_2)$ (**2a/2b**). X-ray structural studies of compounds **1b** and **2a** revealed minimal changes in the coordination sphere of the Ru_2 core. Voltammetric measurements showed that compounds **1** exhibit three one-electron redox processes: a reversible reduction of Ru_2 , a reversible oxidation of Ru_2 , and a quasi-reversible oxidation of an amino group. Compounds **2** display the same Ru_2 -based redox processes but not the $-\text{NH}_2$ oxidation. Compounds **1a/1b** were successfully converted to the corresponding diazonium salts $[\text{Ru}_2(\text{Xap})_4(\text{C}\equiv\text{C}-\text{C}_6\text{H}_4-4-\text{N}_2)](\text{BF}_4)$ (**3a/3b**) via oxidation by nitrosonium tetrafluoroborate, which was generated in situ from *t*-BuONO and BF_3 . However, the attempt to convert compounds **2** to the corresponding diazonium salts was unsuccessful. DFT calculations of model compounds were performed to rationalize some unusual structural and electrochemical characteristics observed for compounds **1/2**.

Introduction

The continuous scaling of Si-based CMOS transistors has become increasingly challenging due to the materials limitation such as the lack of effective dielectric materials at nanometer scale, and hybrid transistors based on the combination of organic molecules and Si-based CMOS devices has been speculated as a promising alternative.¹ As an essential starting point for molecule-CMOS hybrids, covalent attachment of organic molecules to both flat and porous Si surfaces has received intense interest from both chemists and engineers during the last two decades.^{2–4} This is typically accomplished on the basis of a H-passivated Si surface that is produced by etching of the native SiO_2 layer with a solution of HF or NH_4F .^{3,4} Organic molecules with terminal functional groups such as alkynes, alkenes, or diazonium can be grafted onto a H-Si surface under thermal, photochemical, or electrochemical conditions.^{3,5} Recently, the laboratories

of Tour and Paul succeeded in immobilizing polyoxo cluster (Mo_6)⁶ and Fe or Fe/Ru phenylacetylide complexes,⁷ respectively, on p-type H-Si surfaces, demonstrating the feasibility of functionalization with inorganic/organometallic species.

There has been a sustained interest in using metal alkynyl compounds as molecular wires, active components of molecular devices, or electro-optical materials from many laboratories around the world.^{8,9} Efforts from our laboratory focus on diruthenium alkynyl compounds,¹⁰ and both wire characteristics and conductance switching have been documented.¹¹

(7) Gauthier, N.; Argouarch, G.; Paul, F.; Humphrey, M. G.; Toupet, L.; Ababou-Girard, S.; Sabbah, H.; Hapiot, P.; Fabre, B. *Adv. Mater.* **2008**, *20*, 1952.

(8) Paul, F.; Lapinte, C. *Coord. Chem. Rev.* **1998**, *178–180*, 431. Joachim, C.; Gimzewski, J. K.; Aviram, A. *Nature* **2000**, *408*, 541. Paul, F.; Lapinte, C., In *Unusual Structures and Physical Properties in Organometallic Chemistry*; Gielen, M.; Willem, R.; Wrackmeyer, B., Eds.; Wiley: West Sussex, 2002. Low, P. J. *Dalton Trans.* **2005**, 2821. Wong, W.-Y.; Ho, C.-L. *Coord. Chem. Rev.* **2006**, *250*, 2627. Wong, W. Y. *Coord. Chem. Rev.* **2007**, *251*, 2400. Gatteschi, D.; Cornia, A.; Mannini, M.; Sessoli, R. *Inorg. Chem.* **2009**, *48*, 3408–3419. Schull, T. L.; Kushmerick, J. G.; Patterson, C. H.; George, C.; Moore, M. H.; Pollack, S. K.; Shashidhar, R. *J. Am. Chem. Soc.* **2003**, *125*, 3202. Getty, S. A.; Engrtrakul, C.; Wang, L.; Liu, R.; Ke, S.-H.; Baranger, H. U.; Yang, W.; Fuhrer, M. S.; Sita, L. R. *Phys. Rev. B* **2005**, *71*, 241401(R). Kim, B.; Beebe, J. M.; Olivier, C.; Rigaut, S.; Touchard, D.; Kushmerick, J. G.; Zhu, X.-Y.; Frisbie, C. D. *J. Phys. Chem. C* **2007**, *111*, 7521. Liu, K.; Wang, X. H.; Wang, F. S. *ACS Nano* **2008**, *2*, 2315. Vitaliano, R.; Fratoddi, I.; Venditti, I.; Roviello, G.; Battocchio, C.; Polzonetti, G.; Russo, M. V. *J. Phys. Chem. A* **2009**, *113*, 14730. Olivier, C.; Costuas, K.; Choua, S.; Maurel, V.; Turek, P.; Saillard, J.-Y.; Touchard, D.; Rigaut, S. *J. Am. Chem. Soc.* **2010**, *132*, 5638.

(9) Wong, K. M.-C.; Hung, L.-L.; Lam, W. H.; Zhu, N.; Yam, V. W.-W. *J. Am. Chem. Soc.* **2007**, *129*, 4350.

(10) Ren, T. *Organometallics* **2005**, *24*, 4854.

(11) Blum, A. S.; Ren, T.; Parish, D. A.; Trammell, S. A.; Moore, M. H.; Kushmerick, J. G.; Xu, G.-L.; Deschamps, J. R.; Pollack, S. K.; Shashidhar, R. *J. Am. Chem. Soc.* **2005**, *127*, 10010. Mahapatro, A. K.; Ying, J.; Ren, T.; Janes, D. B. *Nano Lett* **2008**, *8*, 2131.

*To whom correspondence should be addressed. E-mail: tren@purdue.edu.

(1) *International Technology Roadmap for Semiconductors: Executive Summary* (http://www.itrs.net/Links/2009ITRS/2009Chapters_2009Tables/2009_ExecSum.pdf); 2009. Aswal, D. K.; Lenfant, S.; Guerin, D.; Yakhmi, J. V.; Vuillaume, D. *Anal. Chem. Acta* **2006**, *568*, 84. Gowda, S.; Mathur, G.; Li, Q. L.; Surthi, S.; Misra, V. *IEEE Trans. Nanotech.* **2006**, *5*, 258.

(2) Linford, M. R.; Chidsey, C. E. D. *J. Am. Chem. Soc.* **1993**, *115*, 12631.

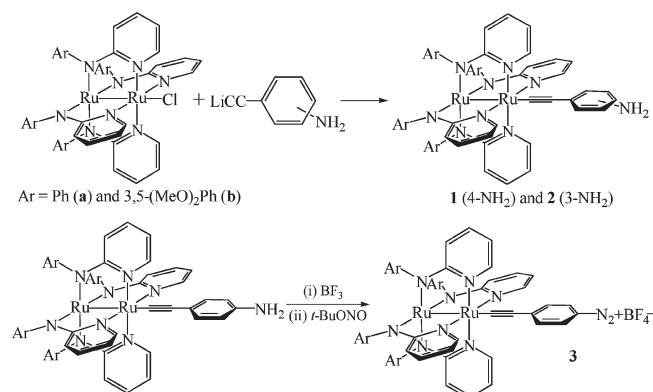
(3) Buriak, J. M. *Chem. Rev.* **2002**, *102*, 1271.

(4) Bent, S. F. *Surf. Sci.* **2002**, *500*, 879.

(5) Stewart, M. P.; Maya, F.; Kosynkin, D. V.; Dirk, S. M.; Stapleton, J. J.; McGuinness, C. L.; Allara, D. L.; Tour, J. M. *J. Am. Chem. Soc.* **2004**, *126*, 370. Tour, J. M. *J. Org. Chem.* **2007**, *72*, 7477.

(6) He, T.; Ding, H. J.; Peor, N.; Lu, M.; Corley, D. A.; Chen, B.; Ofir, Y.; Gao, Y. L.; Yitzchaik, S.; Tour, J. M. *J. Am. Chem. Soc.* **2008**, *130*, 1699. Lu, M.; Nolte, W. M.; He, T.; Corley, D. A.; Tour, J. M. *Chem. Mater.* **2009**, *21*, 442.

Scheme 1. Preparation of Compounds 1–3



Among several types of diruthenium alkyl compounds attainable, those based on Ru₂(ap)₄ (ap is 2-anilino-pyridinate) are particularly attractive due to their rich and robust redox properties, the choice between mono- and bis-alkynylation, and possibility of ligand engineering.^{12–17} Previously, we realized the synthesis of Ru₂(ap)₄-alkynyls with the thiol (–SH) alligator clip,¹⁸ which were used in the said device work through the formation of the Au–S bond.¹¹ Described in this contribution are the preparation of Ru₂(Xap)₄ phenylacetylide compounds containing either a 4- or 3-NH₂ phenyl substituent and the conversion of 4-NH₂ compounds to the corresponding diazonium salts, which can function as an “alligator clip” for the Si surface.

Results and Discussion

Similar to the earlier studies of other Ru₂(ap)₄ monoalkynyl compounds,^{13,16} compounds **1** and **2** were prepared via anion metathesis reactions between Ru₂(Xap)₄Cl and LiC≡CC₆H₄-NH₂ (in slight excess) as outlined in Scheme 1. Purification via silica column using CH₂Cl₂–hexanes resulted in compounds **1** and **2** as dark purple and green microcrystalline solids, respectively, in yields of 60–85%. Both compounds **1** and **2** are paramagnetic with effective magnetic moments between 3.5 and 3.9 μ_B, which are consistent with a ground state of *S* = 3/2.

The diazonium derivatives **3** were prepared using a procedure modified from that of Doyle and Bryker:¹⁹ to a THF solution containing **1** was added boron trifluoride diethyl etherate, followed by *tert*-butyl nitrite, which resulted in the precipitation of diazonium salts **3**.

(12) Chakravarty, A. R.; Cotton, F. A. *Inorg. Chim. Acta* **1986**, *113*, 19.

(13) Zou, G.; Alvarez, J. C.; Ren, T. *J. Organomet. Chem.* **2000**, *596*, 152.

(14) Ren, T.; Zou, G.; Alvarez, J. C. *Chem. Commun.* **2000**, 1197. Ren, T. *Organometallics* **2002**, *21*, 732. Xu, G.-L.; Zou, G.; Ni, Y.-H.; DeRosa, M. C.; Crutchley, R. J.; Ren, T. *J. Am. Chem. Soc.* **2003**, *125*, 10057. Shi, Y.; Yee, G. T.; Wang, G.; Ren, T. *J. Am. Chem. Soc.* **2004**, *126*, 10552. Bear, J. L.; Li, Y.; Han, B.; Caemelbecke, E. V.; Kadish, K. M. *Inorg. Chem.* **1997**, *36*, 5449. Kadish, K. M.; Phan, T. D.; Wang, L.-L.; Giribabu, L.; Thuriere, A.; Wellhoff, J.; Huang, S.; Caemelbecke, E. V.; Bear, J. L. *Inorg. Chem.* **2004**, *43*, 4825. Nguyen, M.; Phan, T.; Caemelbecke, E. V.; Kajonkijya, W.; Bear, J. L.; Kadish, K. M. *Inorg. Chem.* **2008**, *47*, 7775.

(15) Xu, G.-L.; Ren, T. *Organometallics* **2001**, *20*, 2400.

(16) Xu, G.-L.; Cordova, A.; Ren, T. *J. Cluster Sci.* **2004**, *15*, 413.

(17) Xi, B.; Xu, G.-L.; Ying, J.-W.; Han, H.-L.; Cordova, A.; Ren, T. *J. Organomet. Chem.* **2008**, *693*, 1656.

(18) Ren, T.; Parish, D. A.; Xu, G.-L.; Moore, M. H.; Deschamps, J. R.; Ying, J.-W.; Pollack, S. K.; Schull, T. L.; Shashidhar, R. J. *Organomet. Chem.* **2005**, *690*, 4734.

(19) Doyle, M. P.; Bryker, W. J. *J. Org. Chem.* **1979**, *44*, 1572.

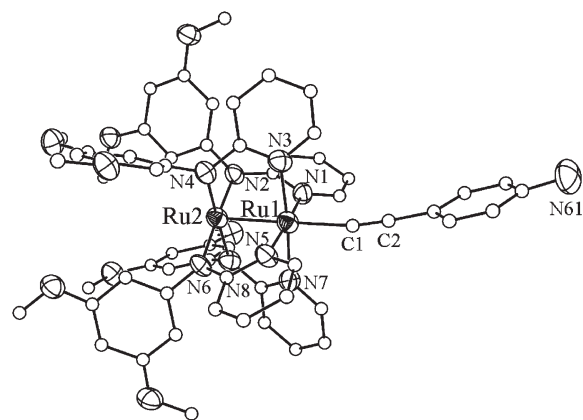


Figure 1. Structural plot of compound **1b**. Hydrogen atoms were omitted for clarity. Selected bond lengths (Å): Ru1–Ru2, 2.329(10); Ru1–C1, 2.097(10); Ru1–N_{av}, 2.093(7); Ru2–N_{av}, 2.022(7); C1–C2, 1.178(14); C2–C3, 1.470(16). Bond angles (deg): Ru2–Ru1–C1, 178.9(2); Ru1–C1–C2, 168.4(8); C1–C2–C3, 176.5(11).

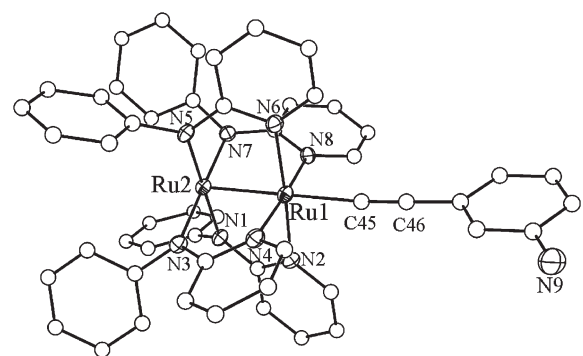


Figure 2. Structural plot of compound **2a**. Hydrogen atoms were omitted for clarity. Selected bond lengths (Å): Ru1–Ru2, 2.3420(5); Ru1–C45, 2.094(6); Ru1–N_{av}, 2.105[5]; Ru2–N_{av}, 2.037[4]; C45–C46, 1.217(8). Bond angles (deg): Ru2–Ru1–C45, 178.58(16); Ru1–C45–C46, 174.2(5); C45–C46–C47, 178.9(7).

The molecular structures of both compounds **1b** and **2a** were determined using X-ray single-crystal diffraction, and their structural plots are presented in Figures 1 and 2, respectively. Both compounds were crystallized in the space group *P* $\bar{1}$, and the asymmetric unit contains one independent molecule in the case of **1b** and two in the case of **2a**. Both independent molecules in **2a** exhibit very similar geometric parameters, and only one is shown in Figure 2.

It is clear from Figures 1 and 2 that the coordination geometry around the Ru₂ core in both **1b** and **2a** is very similar to those determined earlier for related Ru₂(ap)₄-(C≡CR) compounds.^{10,20} In particular, the Ru–Ru (2.329(10)/2.3420(5) Å for **1b/2a**) and Ru–C (2.097(10)/2.094(6) Å for **1b/2a**) bond lengths are the same as those reported for Ru₂(ap)₄(C≡CPh) within experimental error.¹² The average Ru1–N(pyridyl) and Ru2–N(anilino) bond lengths for both **1b** and **2a** are comparable to those tabulated for other related Ru₂(ap)₄(C≡CR) compounds.¹⁰

A curious feature about **1b** is the significant deviation of the Ru1–C1–C2 linkage from linearity, which results in an apparent bend of the 4-NH₂C₆H₄ ring from the

(20) Ren, T.; Xu, G.-L. *Comments Inorg. Chem.* **2002**, *23*, 355.

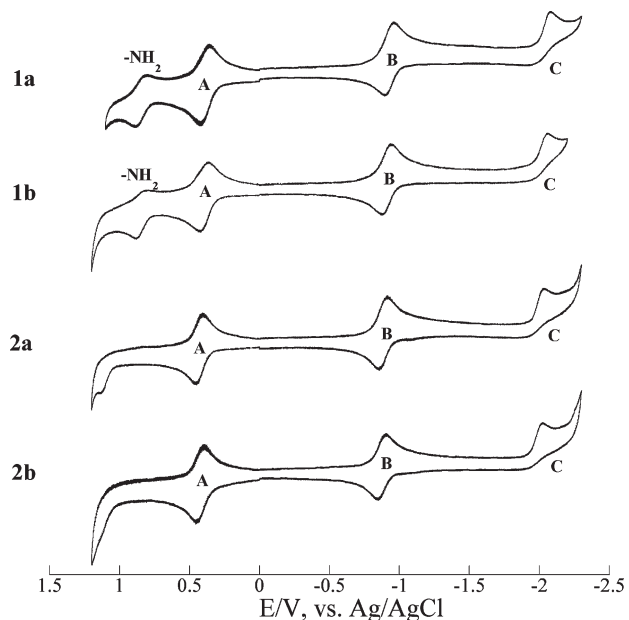


Figure 3. CVs of compounds **1** and **2** recorded in THF at a scan rate of 0.10 V/s.

Ru2–Ru1–C1 axis (Figure 1). In contrast, the Ru1–C45–C46 angle in **2a** ($174.2(5)^\circ$) is more in line with typical Ru–C $_{\alpha}$ –C $_{\beta}$ (175° or higher) angles found for other Ru $_2$ -(*ap*) $_4$ (C≡CR) compounds.^{10,20} Inspection of the packing diagram of **1b** did not reveal any significant intermolecular interaction involving the 4-NH $_2$ C $_6$ H $_4$ ring, hinting that the bend may have an electronic origin. Structural examples of metal– σ -arylacetylides containing –NH $_2$ aryl substituent are sparse, and entries found in the CSD include those of the 4-NH $_2$ substituent with M as Pt,²¹ Au,^{9,22} Fe,^{23,24} and Ru²⁵ and those of the 2-NH $_2$ substituent with M as Pt²⁶ and Re.²⁷ There is no reported structure for the [M]–C≡C–C $_6$ H $_4$ –3-NH $_2$ type. In most of the cases, the nonlinearity of M–C $_{\alpha}$ –C $_{\beta}$ linkage is small but noticeable from the structural plots and typically went unnoticed by the authors. Exceptions to this are the detailed and thorough studies of the M^{II}–C≡C–C $_6$ H $_4$ –4-X series (M = Fe and Ru) by Paul and Lapinte,^{23,25} where a significant bend in the M–C $_{\alpha}$ –C $_{\beta}$ linkage was noticed for compounds with both the electron donor (NH $_2$) and acceptor (NO $_2$) substituents.

Similar to the established Ru $_2$ (*ap*) $_4$ (C≡CR) compounds, compounds **1** and **2** display rich redox chemistry with three one-electron waves attributed to the Ru $_2$ center: a reversible oxidation (A, Ru $_2$ (II,III) to Ru $_2$ (III,III)), a reversible reduction (B, Ru $_2$ (II,III) to Ru $_2$ (II,II)), and subsequent irreversible reduction (C, Ru $_2$ (II,II) to Ru $_2$ (II,I)), as shown in Figure 3. The irreversibility of couple C is due to the dissociation of the axial acetylide ligand upon the second

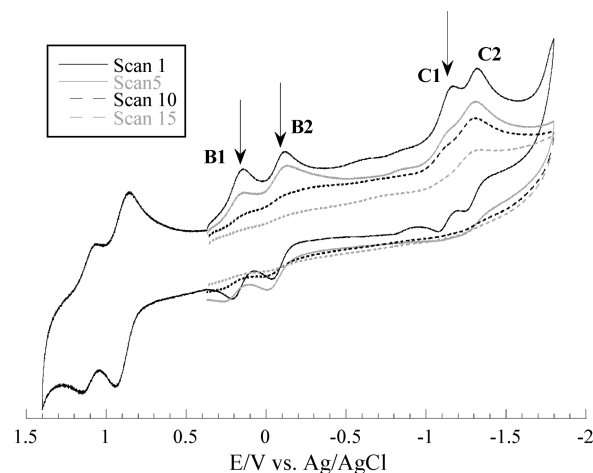


Figure 4. CV of compound **3a** recorded in MeCN at a scan rate of 0.10 V/s. The cathodic region was scanned continuously.

reduction.¹⁰ For compounds **1a/b**, there is an additional quasi-reversible oxidation around 0.88 V that is attributed to the 4-NH $_2$ group. The corresponding peak, however, was not observed for compounds **2** within the potential window allowed by THF. Voltammetric measurements conducted in CH $_2$ Cl $_2$, which allows for a more positive potential window, did not reveal a NH $_2$ oxidation either. It is obvious from Figure 3 that the CVs of **1a** and **1b** are nearly identical, and the same is true about those of **2a** and **2b**. This is consistent with the fact that the substitution on the anilino ring causes very minimal change in the electronic properties of Ru $_2$ (*Xap*) $_4$ species.^{16,17} Examination of $E_{1/2}$ data also reveals that the peaks attributed to Ru $_2$ in **2** are generally 20–40 mV more positive than those in **1**, which is due to the weaker electron-donating ability of 3-NH $_2$ (Hammett constant $\sigma(3\text{-NH}_2) = -0.09$) than that of 4-NH $_2$ ($\sigma(4\text{-NH}_2) = -0.30$).

Diazonium salts are generally prone to quick degradation when subjected to demanding techniques such as MS and elemental analysis. An ESI-MS study of **3a** led to the observation of only fragments (see the Experimental Section below). Hence, diazonium salts are often characterized with IR and ^1H NMR.⁶ Although the paramagnetic nature of **3** prevents a meaningful NMR study, FT-IR of **3** revealed the characteristic N=N stretch at 2228 cm $^{-1}$. Voltammetric measurement of **3**, shown in Figure 4 for **3a**, also offers some insight and indirect proof of the presence of diazonium. For the diazonium salt **3a**, its open circuit potential (OCP) is shifted by +0.37 V from that of **1a**. The anodic region features a reversible oxidation and a quasi-reversible oxidation. The initial scan of the cathodic region revealed four quasi-reversible reductions, labeled as B1, B2, C1, and C2. Interestingly, the first three waves gradually diminished when the CV was scanned continuously (Figure 4), while C2 remains throughout. This type of behavior is expected for a diazonium species: waves B1, B2, and C1 originate from **3a** and disappear as **3a** degrades under electrolytic conditions; wave C2 is likely due to a degradation product that deposits on the glassy carbon working electrode.

Both compounds **1** and **2** exhibit two intense peaks with peak maxima at 480–488 and 744–770 nm, as shown in Figure 5, and this feature is consistent with the prior studies of related Ru $_2$ (*ap*) $_4$ (C≡CR)-type compounds.^{10,13,15,17,28}

(21) Deeming, A. J.; Hogarth, G.; Lee, M.-y. V.; Saha, M.; Redmond, S. P.; Phetmung, H. T.; Orpen, A. G. *Inorg. Chim. Acta* **2000**, *309*, 109.

(22) Hogarth, G.; Álvarez-Falcón, M. M. *Inorg. Chim. Acta* **2005**, *358*, 1386.

(23) Costuas, K.; Paul, F.; Toupet, L.; Halet, J.-F.; Lapinte, C. *Organometallics* **2004**, *23*, 2053.

(24) Paul, F.; Toupet, L.; Thepot, J. Y.; Costuas, K.; Halet, J. F.; Lapinte, C. *Organometallics* **2005**, *24*, 5464.

(25) Paul, F.; Ellis, B. G.; Bruce, M. I.; Toupet, L.; Roisnel, T.; Costuas, K.; Halet, J.-F.; Lapinte, C. *Organometallics* **2006**, *25*, 649.

(26) Fratoddi, I.; Delfini, M.; Sciubba, F.; Hursthouse, M. B.; Ogilvie, H. R.; Russo, M. V. *J. Organomet. Chem.* **2006**, *691*, 5920.

(27) Liddle, B. J.; Lindeman, S. V.; Reger, D. L.; Gardinier, J. R. *Inorg. Chem.* **2007**, *46*, 8484.

(28) Zhang, L.; Xi, B.; Liu, I. P. C.; Choudhuri, M. M. R.; Crutchley, R. J.; Updegraff, J. B.; Protasiewicz, J. D.; Ren, T. *Inorg. Chem.* **2009**, *48*, 5187.

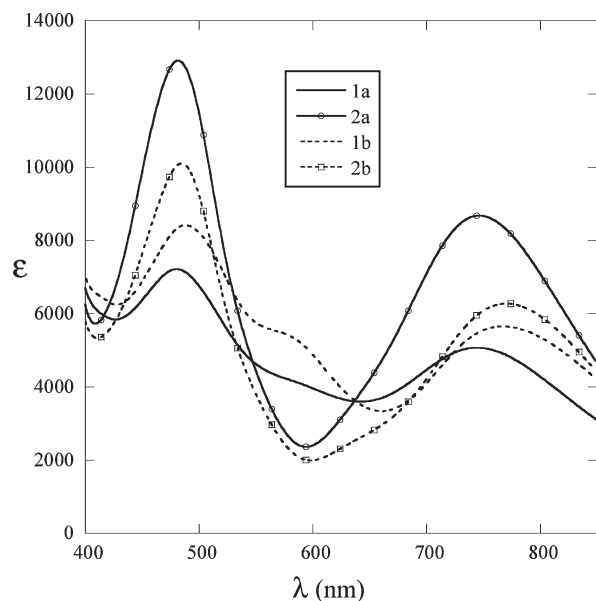


Figure 5. Vis-NIR spectra of compounds **1** and **2** recorded in THF.

On the basis of our recent TD-DFT study of a model compound,²⁸ the higher energy peak is assigned to the transition to the $\delta^*(\text{Ru-Ru})$ orbital from both the $\pi(\text{Ru-Ru})$ and $\pi(\text{Ru-N})$ orbitals, while the lower energy peak is primarily the $\pi(\text{C}\equiv\text{C})$ to $\delta^*(\text{Ru-Ru})$ transition. Both compounds **1a** and **1b** also exhibit a broad shoulder trailing off the high-energy band, which is absent in the spectra of both compounds **2** and other $\text{Ru}_2(\text{ap})_4(\text{C}\equiv\text{CR})$ -type compounds studied earlier. This feature perhaps accounts for the purple color of **1** in THF, which is distinctly different from the brown color of other $\text{Ru}_2(\text{ap})_4(\text{C}\equiv\text{CR})$ -type compounds including **2**. The appearance of this shoulder is likely due to the lone pair of *p*- NH_2 , although the exact nature of the transition remains unclear. The visible region of the absorption spectrum of **3a** (Supporting Information) features a single peak at 676 nm. The contrast between the spectral features of compounds **1** and **3** reflects a significant stabilization of both the $\pi(\text{Ru-Ru})$ and $\pi(\text{C}\equiv\text{C})$ orbitals by the diazonium group, which blue-shifts the band from around 750 nm in **1** to 676 nm in **3**, and the high-energy peak around 480 nm in **1** into the UV region.

Because of the interest in using compounds **1** and **2** as the precursors for molecule-CMOS hybrid devices, we are particularly interested in their electronic structures. Seeking the possible electronic origins of several peculiar experimental observations, such as the bend of the $-\text{CCC}_6\text{H}_4\text{-4-NH}_2$ fragment and the difficulty in oxidizing the 3- NH_2 derivative, DFT calculations were performed on the models for compounds **1** and **2**, namely, model **1**, model **1'**, and model **2**. The geometries of model **1** and model **2** were optimized from the crystal structures of **1b** and **2a**, respectively, with the only simplification being the replacement of anilino methoxy substituents with H atoms in the former. The bond lengths and angles around the Ru_2 core in the optimized geometries match well with those from the crystal structures, and they are given in the Supporting Information. The geometry of model **1'** was idealized from that of model **1** by restricting both Ru-Ru-C_α and $\text{Ru-C}_\alpha\text{-C}_\beta$ to 180° .

It is well established on the basis of the room-temperature effective magnetic moment that the $\text{Ru}_2(\text{ap})_4(\text{C}\equiv\text{CR})$ -type compounds have an $S = 3/2$ ground state.¹⁰ Consistent with

our prior DFT study of a related model compound,²⁸ spin-unrestricted DFT calculations for model **1**, model **1'**, and model **2** all converged to the same configuration with HOMO, HOMO-1, and HOMO-2 being energetically close and singly occupied. The computed molecular orbital diagrams for the three model compounds are shown in Figure 6.

It is clear from Figure 6 that the HOMO of model **1** is predominantly the $\delta^*(\text{Ru-Ru})$ orbital with an additional contribution from the $\pi^*(\text{py})$. The HOMO-1 is primarily made of the *antibonding* combination of $\pi^*(\text{Ru-Ru})$ and $\pi(\text{C}\equiv\text{C})$ orbitals, while the HOMO-2 is an even mix between the *antibonding* combination of $\pi^*(\text{Ru-Ru})$ and $\pi(\text{C}\equiv\text{C})$ orbitals and the π^* orbitals of both pyridinyl and anilino rings. Clearly, the π -interactions between the Ru_2 core and axial acetylide are dominated by the filled-filled type first proposed by Lichtenberger.²⁹ The DFT results of model **1** unambiguously confirm the ground-state configuration of $\sigma^2\pi^4\delta^2\pi^*2\delta^*1$ for the $\text{Ru}_2(\text{II,III})$ core.^{10,30} The LUMO of model **1** is largely a combination of the π^* orbitals of four pyridinyl rings and the $d_{x^2-y^2}$ orbital of $\text{Ru}(\text{py})$, while an early study resulted in a LUMO of $\sigma^*(\text{Ru-Ru})$ nature.²⁸ The discrepancy is likely due to the oversimplification in the early calculation, where all anilino rings were replaced by methyl groups and arylacetylide was replaced by simple acetylide ($-\text{C}\equiv\text{CH}$). The DFT calculation of model **1'** yielded results, both the make up and energies of the frontier MOs, nearly identical to those of model **1**. The only subtle difference is that the energy of HOMO-1 in model **1'** is 0.03 eV higher than that in model **1**.

As shown in Figure 6, the frontier orbitals of model **2** are similar to those of model **1** in both energies and general composition, and the occupancy conforms to a $\pi^*2\delta^*1$ configuration. Nevertheless, there exists a significant contrast in both the HOMO-1 and HOMO-2 orbitals between the two models. In model **1**, the lone pair of 4- NH_2 contributes significantly to both orbitals through the mixing with the aryl π orbitals. On the other hand, contributions from both the lone pair of 3- NH_2 and the aryl π orbitals are hardly noticeable in the HOMO-1 and HOMO-2 orbitals of model **2**. Instead, the π^* orbitals from both pyridyls and anilino rings make up a significant portion of HOMO-1 and HOMO-2. The absence of $-\text{NH}_2$ contribution indicates that the lone pair of the 3- NH_2 group is deeply buried, making its oxidation energetically challenging.

In the course of investigating many $[\text{M}^{\text{II}}]\text{-C}\equiv\text{C-C}_6\text{H}_4\text{-4-X}$ ($\text{M} = \text{Fe}$ and Ru) type compounds, Lapinte and co-workers proposed that the quinoidal resonance structure (analogous to **B** in Scheme 2) may contribute significantly to the electronic properties of metal-acetylide species in addition to the traditional arylacetylide structure (**A** in Scheme 2) with $\text{X} = \text{NH}_2$.^{23-25,31} This classical valence bond (VB) description is clearly applicable to our compounds **1a/1b**, as corroborated by the N-lone pair contribution to both the HOMO-1 and HOMO-2 from the model **1** calculation. The classical VB theory also suggests that a significant contribution by the 3- NH_2 lone pair would invoke a higher

(29) Lichtenberger, D. L.; Renshaw, S. K.; Bullock, R. M. *J. Am. Chem. Soc.* **1993**, *115*, 3276. Lichtenberger, D. L.; Renshaw, S. K.; Wong, A.; Tagge, C. D. *Organometallics* **1993**, *12*, 3522.

(30) Angaridis, P. In *Multiple Bonds between Metal Atoms*; Cotton, F. A.; Murillo, C. A.; Walton, R. A., Eds.; Springer Science and Business Media, Inc.: New York, 2005.

(31) Denis, R.; Toupet, L.; Paul, F.; Lapinte, C. *Organometallics* **2000**, *19*, 4240.

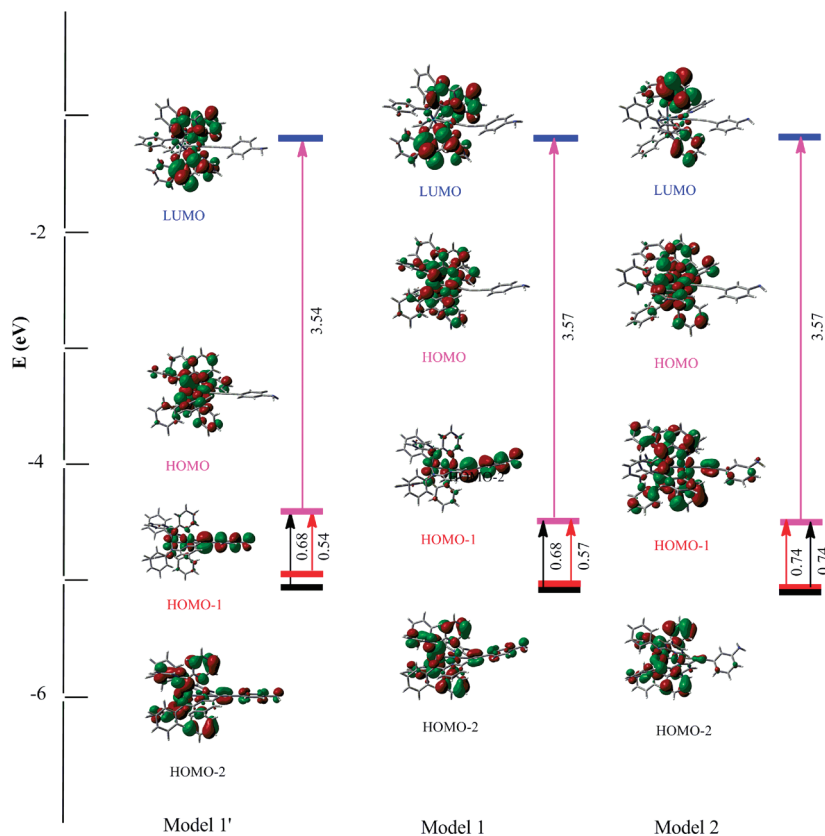
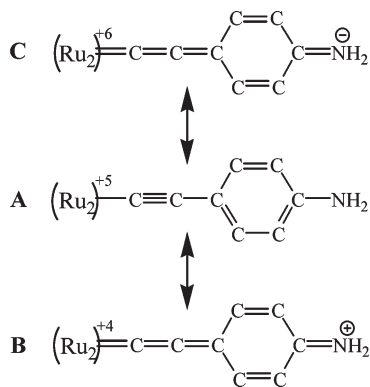


Figure 6. Molecular orbital diagrams for model 1, model 1', and model 2 obtained from DFT calculations.

Scheme 2. Resonance Structures Available to Compounds 1



energy non-Kekulé-type resonance structure,³² and hence is energetically unfavorable. This is again confirmed by the absence of the N-lone pair contribution to either the HOMO-1 and HOMO-2 from the model 2 calculation. The other possible quinoidal structure, C, is less likely for neutral 1, but contributes to the stabilization of the cation upon $-NH_2$ oxidation. The unavailability of such a resonance structure for the 3- NH_2 species (2) may explain the difficulty in oxidizing 3- NH_2 .

Conclusion

Several diruthenium arylacetylide compounds with 4-/3- NH_2 substituents have been prepared and characterized. The 4- NH_2 species can be readily converted to the corresponding diazonium

3 using *tert*-butyl nitrite as the oxidant. The 3- NH_2 analogues cannot be converted similarly. The contrast between two compounds was rationalized based on DFT studies. Currently, the grafting of 3 onto H-Si surfaces is being explored in our laboratory.

Experimental Section

General Procedures. Trimethylsilylacetylene (TMS-acetylene) was purchased from GFS Chemicals; $BF_3 \cdot \text{etherate}$, *tert*-butyl nitrite, and *n*-BuLi (2.5 M in hexanes) were purchased from Aldrich. THF was distilled over Na/benzophenone under an N_2 atmosphere. $Ru_2(ap)_4Cl$,¹³ $Ru_2(DiMeOap)_4Cl$,¹⁷ 1-amino-4-trimethylsilylethynylbenzene,³³ and 1-amino-3-trimethylsilylethynylbenzene³⁴ were prepared according to literature procedures. 1-Amino-4-trimethylsilylethynylbenzene and 1-amino-3-trimethylsilylethynylbenzene were deprotected via K_2CO_3 in MeOH-THF. All reactions were done using Schlenk techniques under nitrogen and monitored by TLC with EtOAc-hexanes (v/v, 3:7). UV-vis-NIR spectra were obtained with a JASCO V-670 UV-vis-NIR spectrophotometer. Infrared spectra were obtained on a JASCO FT-IR 6300 spectrometer via ATR on a ZnSe crystal. Magnetic susceptibility data were measured at 293 K with a Johnson Matthey Mark-1 magnetic susceptibility balance. Elemental analysis was performed by Atlantic Microlab, Norcross, GA. Cyclic voltammograms were recorded in 0.2 M *n*-Bu₄NPF₆ and a 1.0 mM diruthenium species solution (THF, N_2 degassed) on a CHI620A voltammetric analyzer with a glassy carbon working electrode (diameter = 2 mm), a Pt-wire counter electrode, and an Ag/AgCl reference electrode with ferrocene used as an internal reference (0.620 V).

(33) Takahashi, S.; Kuroyama, Y.; Sonogashira, K.; Hagihara, N. *Synthesis* **1980**, 627.

(34) Lavastre, O.; Cabioch, S.; Dixneuf, P. H.; Vohlidal, J. *Tetrahedron* **1997**, 53, 7595.

(32) Borden, W. T.; Iwamura, H.; Berson, J. A. *Acc. Chem. Res.* **1994**, 27, 109.

Preparation of Ru₂(ap)₄-(C₂C₆H₄-4-NH₂) (1a). Ru₂(ap)₄Cl (196 mg, 0.213 mmol), dried under vacuum for 30 h at 80 °C, was dissolved in 25 mL of THF. To the Schlenk flask containing 4-ethynylaniline (50 mg, 0.42 mmol) dissolved in 5 mL of THF was added 200 μL of 2.5 M *n*-BuLi in hexanes (0.50 mmol) at -70 °C. Upon warming to ambient temperature, the lithiated ligand was transferred via cannula to the Ru₂(ap)₄Cl solution. The reaction mixture turned black and was allowed to stir overnight. The reaction mixture was filtered through a silica plug deactivated by 10% v/v TEA-hexanes and purified on a silica column with CH₂Cl₂-hexanes (v/v, 1:10 to 1:2) to yield 169 mg of **1a** as a purple crystalline solid (80% based on Ru). Data for **1a**: *R_f* = 0.22; ESI-MS, [M]⁺, 996.16; visible spectra, λ_{max} (nm, ε (M⁻¹ cm⁻¹)) 484(7200), 744(5200); IR (cm⁻¹) NH₂ 3377(m), C≡C 2033(m). Anal. Calcd for Ru₂C₅₂H₄₂N₉O₃ (1a·2THF·1H₂O) (found): C, 62.27 (62.50); H, 5.23 (5.18); N, 10.89 (10.56). Cyclic voltammogram [*E*_{1/2}/V, Δ*E*_p/V, *i*_{backward}/*i*_{forward}]: *E*_{pa}(-NH₂), 0.882; **A**, 0.389, 0.031, 0.80; **B**, -0.931, 0.033, 0.81; *E*_{pc}(C), -2.082. μ_{eff}: 3.57 μ_B.

Preparation of Ru₂(ap)₄-(C₂C₆H₄-3-NH₂) (2a). The synthesis of **2a** followed the procedure for **1a** using 1.38 g of Ru₂(ap)₄Cl (1.51 mmol), 295 mg (2.52 mmol) of *m*-ethynylaniline, and 1.0 mL of 2.5 M *n*-BuLi. After filtering through a silica pad the residue was loaded onto deactivated silica gel and eluted via hexanes-EtOAc-Et₃N beginning with 20:1:0.1 and slowly increasing EtOAc to 2:1:0.01, yielding 940 mg (63%) of brown material. Data for **2a**: *R_f* = 0.20; ESI-MS, [M]⁺, 996.16; visible spectra, λ_{max} (nm, ε (M⁻¹ cm⁻¹)) 480(12900), 748(8700); IR (cm⁻¹) NH₂ 3367(m), C≡C 2047(w). Anal. Calcd for Ru₂C₅₂H₄₂N₉ (found): C, 62.76 (62.95); H, 4.25 (4.15); N, 12.67 (12.64). Cyclic voltammogram [*E*_{1/2}/V, Δ*E*_p/V, *i*_{backward}/*i*_{forward}]: *E*_{pa}(-NH₂), 1.132; **A**, 0.433, 0.027, 0.84; **B**, -0.884, 0.028, 0.84; *E*_{pc}(C), -2.036. μ_{eff}: 3.73 μ_B.

Preparation of Ru₂(diMeOap)₄-(C₂C₆H₄-4-NH₂) (1b). The synthesis and purification of **1b** followed the procedure for **1a** using 580 mg (0.501 mmol) of Ru₂(diMeOap)₄Cl, 139 mg (1.19 mmol) of *p*-ethynylaniline, and 500 μL (1.25 mmol) of 2.5 M *n*-BuLi to yield 400 mg (65%) of a purple solid. Data for **1b**: *R_f* = 0.08; ESI-MS, [M]⁺, 1235.30; visible spectra, λ_{max} (nm, ε (M⁻¹ cm⁻¹)) 488(8400), 767(5800); IR (cm⁻¹) NH₂ 3371(m), C≡C 2033(m). Anal. Calcd for Ru₂C₆₈H₈₀N₉O₁₃ (found): C, 58.34 (57.91); H, 4.73 (4.69); N, 10.20 (9.90). Cyclic voltammogram [*E*_{1/2}/V, Δ*E*_p/V, *i*_{backward}/*i*_{forward}]: *E*_{pa}(-NH₂), 0.878; **A**, 0.393, 0.026, 0.73; **B**, -0.907, 0.030, 0.94; *E*_{pc}(C), -2.067. μ_{eff}: 3.79 μ_B.

Preparation of Ru₂(diMeOap)₄-(C₂C₆H₄-3-NH₂) (2b). The synthesis and purification of **2b** followed the procedure for **1a** using 150 mg (0.132 mmol) of Ru₂(diMeOap)₄Cl, 22 mg (0.188 mmol) of *m*-ethynylaniline, and 90 μL (0.225 mmol) of 2.5 M *n*-BuLi to yield 120 mg (75%) of a brown solid. Data for **2b**: *R_f* = 0.12; ESI-MS, [M]⁺, 1235.30; visible spectra, λ_{max} (nm, ε (M⁻¹ cm⁻¹)) 485(10100), 770(6300); IR (cm⁻¹) NH₂ 3371(m), C≡C 2048(w). Anal. Calcd for Ru₂C₆₀H₅₈N₉O₈ (found): C, 58.34 (57.91); H, 4.73 (4.69); N, 10.20 (9.90). Cyclic voltammogram [*E*_{1/2}/V, Δ*E*_p/V, *i*_{backward}/*i*_{forward}]: **A**, 0.424, 0.031, 0.96; **B**, -0.872, 0.033, 0.87; *E*_{pc}(C), -2.026. μ_{eff}: 3.81 μ_B.

Preparation of [Ru₂(ap)₄-(C₂C₆H₄-4-N₂)]BF₄ (3a). In a three-neck flask 100 mg (0.100 mmol) of compound **1a** was dissolved in 6 mL of THF and placed in a dry ice-acetone bath. In a Schlenk tube 350 μL (3.22 mmol) of BF₃·Et₂O was diluted in 10 mL of Et₂O and cooled in a dry ice-acetone bath, then transferred to the three-neck flask via cannula. The mixture was stirred for 45 min, turning brown. The three-neck flask was then placed at room temperature, and 325 μL (2.06 mmol) of *t*-BuNO₂ was added and stirred until a precipitate formed. The mixture was filtered through a double male frit and the solid placed on high vacuum to yield 107 mg of a dark green solid

(96.9%). Data for **3a**: ESI-MS, 878.7[M - CC - Ph - N₂⁺BF₄⁻]⁺, 903.0[M - Ph - N₂⁺BF₄⁻]⁺, 1007.9[M - BF₄⁻]⁺; visible spectra, λ_{max} (nm, ε (M⁻¹ cm⁻¹)) 668(16000); IR (cm⁻¹) N=N 2228 (m), C≡C 2131 (m). Cyclic voltammogram in MeCN: *E*_{pa}/V: 1.145, 0.940, *E*_{pc}/V: 0.140, -0.120, -1.158, 1.313, -1.81 (*E*_{1/2}(Fc⁺/Fc): 0.430 V; open circuit potential 0.37 V).

Preparation of [Ru₂(diMeOap)₄-(C₂C₆H₄-4-N₂)]BF₄ (3b). The synthesis followed the same procedure as that for **3a** using 72.3 mg of **1b** in 5 mL of THF. The diazonium salt was obtained in quantitative yield. Data for **3b**: visible spectra, λ_{max} (nm, ε (M⁻¹ cm⁻¹)) 681(11000); IR (cm⁻¹) N=N 2228 (m), C≡C 2111 (m). Cyclic voltammogram in MeCN: *E*_{pa}/V 1.128, 0.976, *E*_{pc}/V 0.117; -0.083; -1.101; -1.289 (*E*_{1/2}(Fc⁺/Fc): 0.414 V; open circuit potential 0.30 V).

Computational Methods. The full geometry optimizations of structures **1b** and **2a** were based on obtained crystal structures, with **1b** treated as **1a** by removal of the methoxy substituents and using the density functional theory (DFT) method, and were based on the hybrid B3LYP density functional model,³⁵ consisting of the Slater local exchange,³⁶ the nonlocal exchange of Becke,³⁷ the local correlation functional of Vosco-Wilk-Nusair,³⁸ and the nonlocal correlation functional of Lee-Yang-Parr.³⁹ The basis set used for all atoms was the LanL2DZ by considering the involvement of metals. All calculations were carried out with the Gaussian 03 suite of programs.⁴⁰ No negative frequency observed in the vibrational frequency analysis indicates that these aniline-substituted diruthenium complexes are metastable equilibrium structures.

Structure Determination. Single crystals of compounds **1b** and **2a** were grown by slow cooling in a 1:3 mixture of THF-hexanes and vapor-vapor diffusion of pentane into a CH₂Cl₂ solution, respectively. X-ray diffraction data were collected on a Rigaku Rapid II image plate diffractometer using Cu Kα radiation (λ = 1.54184 Å) at 150 K, and the structures were solved using the structure solution program PATTY in DIRDIF99⁴¹ and refined using SHELX-07.⁴² Crystal data for **1b**: C₆₀H₅₈N₉O₈Ru₂·3(C₄H₈O), fw = 1451.6, triclinic, *P* $\bar{1}$, *a* = 13.2318(13) Å, *b* = 13.9353(13) Å, *c* = 21.626(2) Å, α = 105.296(6)°, β = 90.477(8)°, γ = 97.294(8)°, *V* = 3811.6(6) Å³, *Z* = 2, *D*_{calc} = 1.265 g cm⁻³, *R*₁ = 0.087, *wR*₂ = 0.259. Crystal data for **2a**: C₅₂H₄₂N₉Ru₂·CH₂Cl₂, fw = 1080.05, triclinic, *P* $\bar{1}$, *a* = 10.0003(5) Å, *b* = 20.0034(8) Å, *c* = 25.6160(9) Å, α = 74.969(3)°, β = 81.982(4)°, γ = 79.121(4)°, *V* = 4837.8(4) Å³, *Z* = 4, *D*_{calc} = 1.483 g cm⁻³, *R*₁ = 0.059, *wR*₂ = 0.179.

Acknowledgment. We thank the National Science Foundation (Grant No. CHE 0715404) for support.

Supporting Information Available: DFT calculation details for model **1**, model **1'**, and model **2**, voltammograms and vis spectra of compounds **3**, and X-ray crystallographic details (CIF) of **1b** and **2a**. This material is available free of charge via the Internet at <http://pubs.acs.org>.

(35) Becke, A. D. *J. Chem. Phys.* **1993**, *98*, 5648. Stephens, P. J.; Devlin, F. J.; Chabalowski, C. F.; Frisch, M. J. *J. Phys. Chem.* **1994**, *98*, 11623.

(36) Slater, J. C. *The Self-consistent Field for Molecules and Solids, in Quantum Theory of Molecules and Solids*; McGraw Hill: New York, 1974.

(37) Becke, A. D. *Phys. Rev. A* **1988**, *38*, 3098.

(38) Vosko, S. H.; Wilk, L.; Nusair, M. *Can. J. Phys.* **1980**, *58*, 1200.

(39) Lee, C. T.; Yang, W. T.; Parr, R. G. *Phys. Rev. B* **1988**, *37*, 785.

(40) Frisch, M. J.; et al. et al. *Gaussian 03, Revision D.02*; Gaussian, Inc.: Wallingford, CT, 2003.

(41) Beurskens, P. T.; Beurskens, G.; deGelder, R.; Garcia-Granda, S.; Gould, R. O.; Smits, J. M. M. *The DIRDIF2008 Program System*; Crystallography Laboratory, University of Nijmegen: The Netherlands, 2008.

(42) Sheldrick, G. M. *Acta Crystallogr. A* **2008**, *64*, 112.